Electronic Supplementary Information

Anion-Induced Morphological Regulation of $In(OH)_3$ Nanostructures and their Conversion into Porous In_2O_3 Analogues

Qiang Wu,[1,*] Jianxiang Chen,[1] Fan Zhang,[1] Pei Xiao,[1] Yinong Lü,[2] Xizhang Wang,[1] and Zheng Hu[1]

[1] Key Laboratory of Mesoscopic Chemistry of MOE, School of Chemistry and Chemical Engineering, Nanjing University, Nanjing 210093, China
[2] College of Materials Science and Engineering, Nanjing University of Technology, Nanjing 210009, China
* E-mail: wqchem@nju.edu.cn

INDEX:

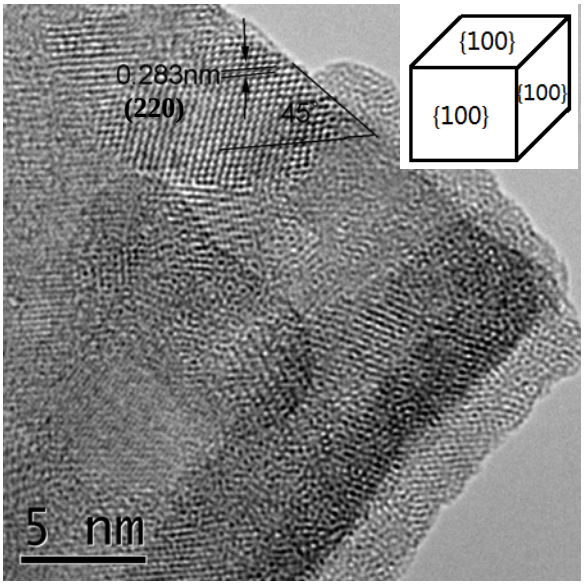

Fig. S1 HRTEM image of $In(OH)_3$ nanocubes. It shows the fringes of (220) lie at an angle of 45° to the nanocube edge, revealing the exposed surfaces of {100} for the nanocubes. The nanocubes seem to have poor crystallinity possible due to the decomposition of $In(OH)_3$ under the irradiation of electron beam. Inset is the schematic illustration of nanocubes.

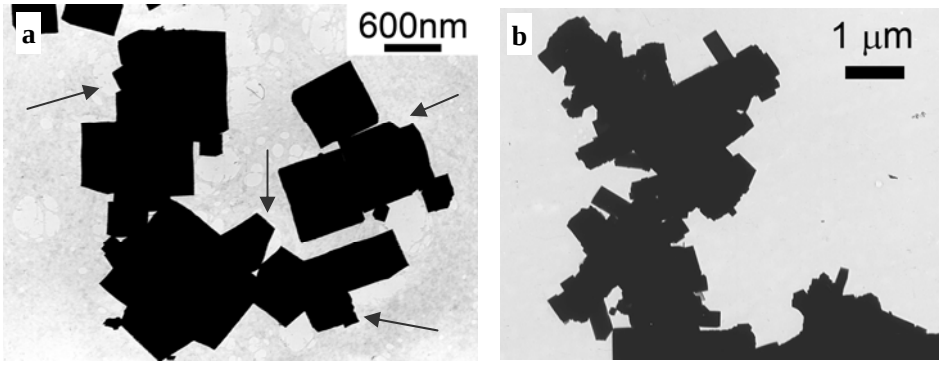

Fig. S2 TEM images of the products obtained without using PVP. (a) without using PVP (b) without using PVP but with PEG. It is seen irregular nanoparticles (Arrows highlight the typical irregular sites on the particles) with large size are produced when PVP is absent, while aggregated nanorods are formed with PEG. These results indicate PVP may act as a dispersive and face-inhibited agent in the synthesis of nanocubes.

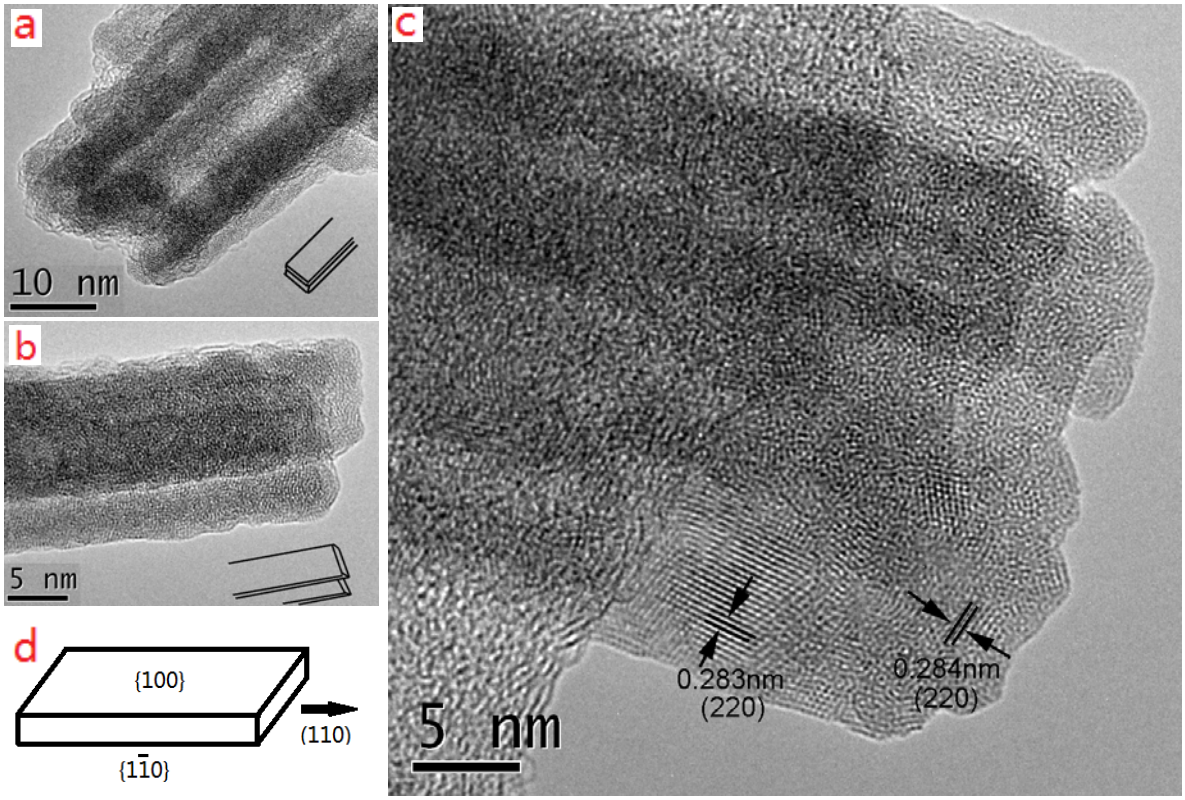

Fig. S3 TEM images and schematic illustration of $In(OH)_3$ nanoflakes. TEM images in (a-c) show that most of the nanostructures are constructed by few (typically two) nanoflakes laminated face-to-face. Two overlap modes, i.e., vertical overlapping and misaligned overlapping, could be usually observed as typically shown in (a) and (b). The driving force for the formation of the overlapped structures is to reduce the surface energies. The crystallinity of the twinned nanoflakes is poor under the irradiation of electron beam. The observed crystalline fringes show the distance of 0.283 nm, corresponding to the (220) planes of $In(OH)_3$. The crystalline structures of the nanoflakes are schematically illustrated in (d), showing the flat surfaces of {100} and side surfaces of {110}. This is also similar to the structures of $In(OH)_3$ thin nanorods reported by Gao et al. [Huang, J. H. Gao, L. Anisotropic Growth of $In(OH)_3$ Nanocubes to Nanorods and Nanosheets via a Solution-Based Seed Method. *Crystal Growth Design* **2006**, *6*, 1528–1532.].

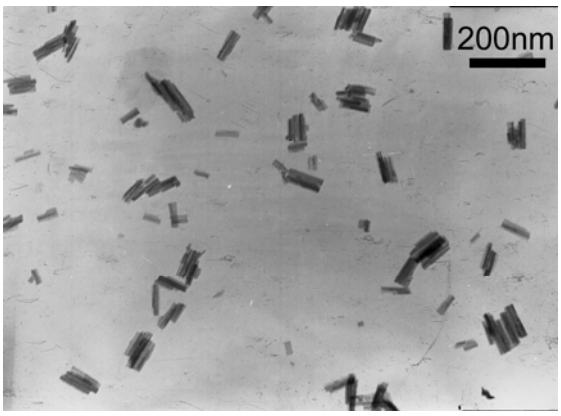

Fig. S4 TEM image of the product obtained with double amount of NO_3^- anions. It is seen just a few nanoflakes are stacked to form the aligned assemblies.

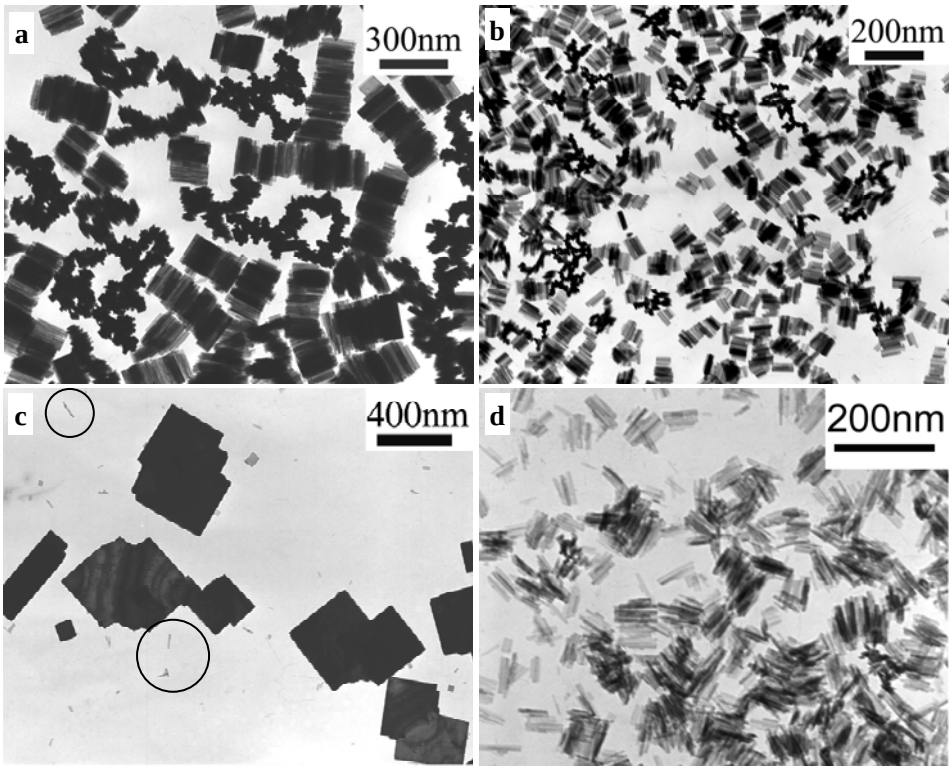

Fig. S5 Influences of indium nitrate concentrations and hydrothermal temperatures on the products. (a,b) TEM images of the $In(OH)_3$ superstructures obtained with 3 mmol and 0.75 mmol of indium nitrate precursor. (c,d) TEM images of the products synthesized at 130 °C and 80 °C.

The concentration of indium nitrate can influence the size of the final products. Using double amount of indium nitrate in the hydrothermal synthesis, the self-assembled superstructures have the widths of about 200 nm and the lengths in the range of 250-1000 nm, obviously larger than those of product no.2 (with 1.5 mmol of indium nitrate) shown in Fig. 1g-h in the main text. When the indium nitrate precursor was decreased to half, aligned assemblies could also be obtained, except that their lengths and widths are significantly reduced. The numbers of the aggregated nanoflakes are much less than those products with higher concentration of indium precursor.

The change in hydrothermal temperature can lead to the morphological transformation for the $In(OH)_3$ product. As shown in Fig. S5c, large nanosheets with zigzag edges form at 130 °C, accompanied with some flakes. These nanosheets are thin as reflected by the image contrast and the interference phenomenon observed on the sheets, showing their good crystallinity. Decreasing the hydrothermal temperature to 80 °C can decrease the aggregation degree of nanoflakes (Fig. S5d), possibly owing to the weak attraction between the twinned nanoflakes under this low temperature.

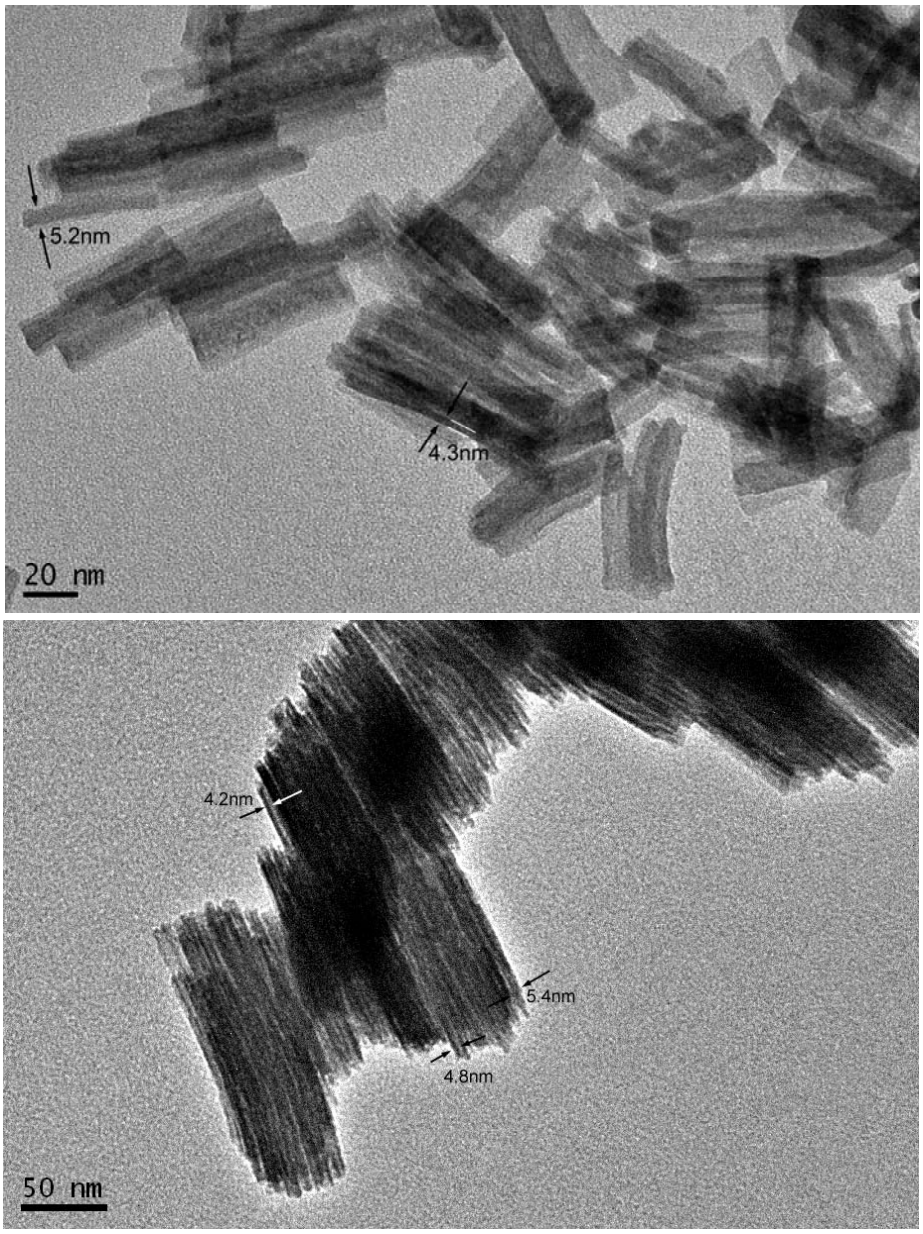

Fig. S6. High resolution TEM images of $In(OH)_3$ nanoflakes and superstructures. As exhibited, the nanoflakes have the thickness of about 5 nm.

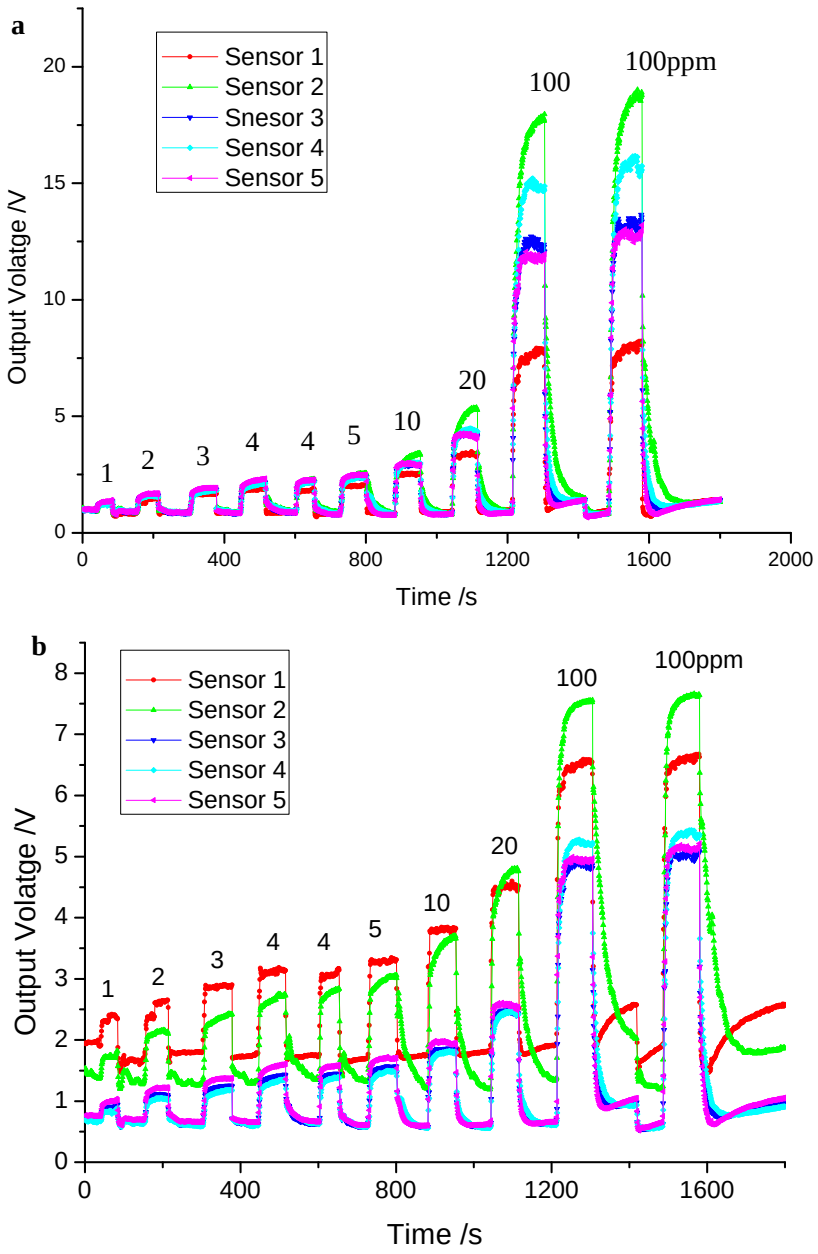

Fig. S7 Response curves of gas sensors. (a) 5 sensors made from porous In_2O_3 superstructures. (b) 5 sensors from porous In_2O_3 nanocubes. The results also indicate that the gas sensors based on the porous In_2O_3 nanostructures show good reversibility and repeatability. The numbers marked on the top of peaks are the corresponding concentrations of ethanol vapor.